Horizontal ramping rate framework to quantify hydropeaking stranding risk for fish

Yann Le Coarer, Marie-hélène Lizée, Leah Beche, Maxime Logez

Received: 3 February 2022 | Revised: 10 November 2022 | Accepted: 14 November 2022

DOI: 10.1002/rra.4087

SPECIAL ISSUE PAPER

WILEY

Horizontal ramping rate framework to quantify hydropeaking stranding risk for fish

Yann Le Coarer[1] | Marie-Hélène Lizée[1] | Leah Beche[2] | Maxime Logez[3]

[1]INRAE, Aix Marseille Univ, RECOVER, Aix-en-Provence, France

[2]CIH, Hydro Engineering Center Service Environnement et Société Savoie Technolac, La Motte Servolex, France

[3]INRAE, UR RIVERLY, Villeurbanne, France

Correspondence
Yann Le Coarer, INRAE, Aix Marseille Univ, RECOVER, Aix-en-Provence, France.
Email: yann.lecoarer@inrae.fr

Abstract

Hydropeaking due to hydropower production can have negative impacts on aquatic fauna. One of the mechanisms for causing impacts on fish and aquatic macroinvertebrates is linked to the rapid dewatering of habitats, which can result in stranding or trapping. The magnitude of these impacts depends both on the characteristics of the flow variations and of the river morphology, as well as biological parameters (species, behavior, etc). When discharge is rapidly reduced, the risk of impacts on fishes (and notably the risk of fish stranding in dewatered zones along the riverbank) is frequently assessed by calculations of vertical ramping velocity among other methods. However, to assess fish stranding risks, the lateral ramping velocity calculated as a horizontal ramping rate (HRR) appears to be a more relevant indicator as it directly measures shoreline drawdown rates. HRR has the advantage of integrating river morphology, but it remains challenging to calculate HRRs in complex situations such as braided rivers. Using hydraulic simulations of the Durance, a gravel bed braided river, we have developed an innovative approach for HRR calculation. Considering two simulated flows, the algorithms for the calculations require partitioning the finite elements into wet and drying meshes. To recommend rates of lowering discharges during hydropeaking events, further studies are required to evaluate more precisely HRR limits for fish stranding regarding biotic and abiotic parameters: species, sizes, nychthemeral cycles, temperature, substrate, and so forth.

KEYWORDS
ecohydraulics, environmental flows, horizontal ramping rate, hydropeaking, mitigation

1 | INTRODUCTION

Continental aquatic ecosystems are heavily affected by continually increasing human needs, as they provide a large variety of ecosystem services on which human societies rely. For instance, rivers provide water for drinking, industry, agriculture, and power generation, as well as being critical to agriculture, flood control, and cultural uses (e.g., Anderson et al., 2019). To respond to these needs, European rivers have been heavily modified, notably by dams, resulting in a very high level of river fragmentation and a reduction of free-flowing sections (e.g., Maaß, Schüttrumpf, & Lehmkuhl, 2021).

Hydropower has consequences on rivers that are generally broader than habitat fragmentation alone. Hydroelectricity production is often associated with alterations in discharge (both water and sediments), often by creating lentic areas upstream of a dam and regulated-flow sections downstream. When a bypassed reach is created, flows in the bypassed reach are diverted for hydroelectric production further downstream, and the diverted water is released further downstream, as a function of energy production needs. The overall management of flows in the entire river is now recognized as being key for maintaining freshwater ecosystem health and human well-being (The Brisbane Declaration, 2007).

The ecological consequences of hydropeaking, discontinuous release of turbined water due to peaks of energy demand (Greimel et al., 2018), have been well documented and their management falls within an environmental flows framework (Lamouroux et al., 2018). Although each river and hydroelectric plant is unique in its functioning, hydropeaking can result in impacts on both the morphological and the ecological functioning of rivers (e.g., Greimel et al., 2018). Indeed, different case studies have illustrated impacts on riparian and aquatic vegetation (e.g., Bejarano, Jansson, & Nilsson, 2017), macroinverterbrates (e.g., Bruno, Siviglia, Carolli, & Maiolini, 2013; Patterson & Smokorowski, 2011; Salmaso, Espa, Crosa, & Quadroni, 2021) (increased drift, reduced abundance, potential for stranding), and also on fishes. One of the major impacts of hydropeaking is fish stranding or trapping when there is a rapid decrease in flow (e.g., Irvine, Thorley, Westcott, Schmidt, & DeRosa, 2015), because fish cannot detect these water level fluctuations as a result of their absence of proprioception but above all because they cannot respond quickly enough to the regressing water edge. This is particularly true for young fish (Irvine et al., 2015). Fish trapping occurs when fishes become trapped in depressions in the riverbed or in secondary channels that become partially or totally disconnected when the water level decreases, thereby creating isolated pools. Fish stranding occurs on riverbanks that are inundated during peaking flows, but which are exposed during lower flows. Fish that cannot detect or respond to the rapid water level changes along the riverbank can become stranded there (e.g., Greimel et al., 2018). However, fish trapping can occur independent of the rapidity of the water level changes (water line recession difficult or impossible to detect in a riverbed depression). In the case of trapping, the main factor influencing its occurrence is the connection/disconnection related to the amplitude between base and peak flows and the specific river morphology.

Fish stranding is highly site- and species-dependent, as well as being related to the hydropeak hydrogram and reach morphology. Numerous factors (e.g., Greimel et al., 2018; Halleraker et al., 2003; Irvine et al., 2015) can influence the stranding risk such as temperature, season; circadian cycle; ramping rates; and the fish size, age, and corresponding behavioural changes (e.g., Hayes et al. 2019). For example, regarding the influence of temperature on stranding risk, fish during cold temperatures fish stay closer to the substrate and their mobility is reduced (lower swimming capacity) during cold temperatures, which increases their stranding risk compared to periods with warmer temperatures.

The role and importance of some of these factors on stranding risk are likely to be species-specific. For example, stranding of cyprinid fishes seems to be similarly influenced by temperature and ramping rates as salmonids are (Bradford, 1997; Halleraker et al., 2003; Harby, Forseth, Ugedal, Bakken, & Sauterleute, 2016; OFEV, 2016; Saltveit, Halleraker, Arnekleiv, & Harby, 2001), indicating that these trends seem robust among different species. Regarding the influence of the nychthemeral cycle, a difference has been shown between the responses of trout and char (Alanärä & Brännäs, 1997; Björnsson, 2001), so it is likely hydropeaking has a different effect on these species and their trophic resources based on their day or night activities.

The Vertical Ramping Rate (VRR) was developed to specifically address the issue of fish stranding during hydropeaking, and to provide a tool for water managers and hydroelectric producers to understand and mitigate these effects (e.g., Hauer, Holzapfel, Leitner, & Graf, 2017). VRR characterizes the vertical ramping velocity, the change in water depth over time between base and peak flows. This concept was first developed for mountainous V-shaped rivers with high slopes and high flows. For such rivers, the vertical ramping velocity is a good surrogate for assessing fish stranding risk, as the river edges are relatively steep. It has been successfully used to modify hydropower operations to reduce hydropeaking impacts on salmonids (Moreira et al., 2019).

Nonetheless, in large rivers with wide active channels such as braided rivers, a small fluctuation of the vertical water level results in a large increase or decrease in the wetted width, and thus the habitat available for small fish (either small species and/or young fish). For such rivers, the change in water surface levels may not reflect the actual stranding risk of young fish (but see Schmutz et al., 2013 which defined VRR thresholds for gravel banks with a lateral gradient of 5%). On the other hand, the horizontal water level variation over time (on the riverbank), the horizontal ramping rate (HRR) or lateral ramping velocity, would better reflect the stranding risk by integrating the effect of channel morphology on water levels. According to several authors, HRR is more relevant because it incorporates the shape of the wetted bed and reflects how far the fish must travel to avoid stranding (Hauer et al., 2017; Schneider & Kopecki, 2016; Tuhtan, Noack, & Wieprecht, 2012). Even though no threshold values currently exist in the ecohydraulics literature to link HRR to stranding risk (Moreira et al., 2019), the tools necessary to calculate HRR and therefore develop such thresholds have also been lacking. Hydraulic two-dimensional models provide local estimations of water depths, velocities at different water discharge, and thus appear to be useful candidate tools from which HRR could be computed, thus enabling it to be tested in future studies of stranding risk.

The main objective of this paper is to present the concept of HRR and the different necessary steps to compute it from a two-dimensional finite element model such as Telemac 2D (Hervouet, 2007). To briefly illustrate the possible outputs of the HRR approach, we used an example taken from a reach of the Durance River (Southeast of France) which is a braided river impacted in its most downstream reach by water level variations that resemble hydropeaking.

2 | METHODS

To evaluate the stranding risk of juvenile fish during hydropeaking events, the HRR indicator, appears to be more universally applicable than the VRR indicator as the latter accounts for riverbed morphology (Figure 1).

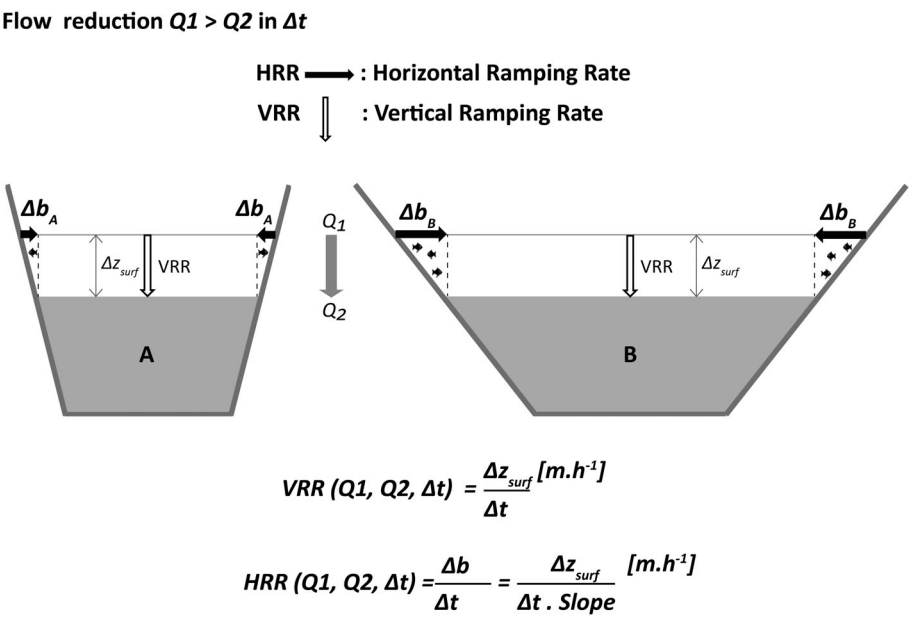

FIGURE 1 Illustration of the difference between the Vertical Ramping Rate (VRR) and Horizontal Ramping Rate (HRR). For the same VRR, the HRR and consequently, the estimated fish stranding risk, differs as a function of river morphology. For a flow reduction of a pair of discharges (*Q1*, *Q2*), Δt is the time interval, Δz is the variation of the water level, and Δb is the local lateral displacement of the shoreline in the horizontal plane

Here we propose a method to calculate the average HRR value in the case of a flow reduction from *Q1* to *Q2* during a time interval Δt from 2D hydraulic simulations. This method can be used even in the complex case of a braided river. It also produces a map of the local HRR values in the dewatered area, making it possible to identify the highest-risk areas to be evaluated in the field.

The case presented here is the use of a 2D finite element hydraulic model with a fixed triangular mesh. The notations used in the equations are defined in the list of symbols at the end of the paper.

In the case of a trapezoidal channel with Δz_{surf} the variation of the water surface level, and a mean horizontal displacement Δb of the shoreline, the HRR equation is:

$$\mathrm{HRR}(Q1, Q2, \Delta t) = \frac{\Delta b}{\Delta t} = \frac{\Delta z_{surf}}{smaxb \cdot \Delta t} \quad (1)$$

To calculate correctly, it is necessary to consider the slope of the river bank. In the case of a hydraulic simulation, the maximum slope of the bottom *smaxb* of a dewatered cell should be used.

Appendix 1 explains how this calculation should be performed. It is the maximum slope that is used by a drop of water that runs down a triangular facet.

Note that in the case of Equation (1), the HRR is calculated as the same for the left bank as well as for the right bank. Note also that Equation (3) below, will provide the correct value of the HRR in the case of our trapezoidal channel, and this regardless of the mesh in the bank that will have been dewatered, because whatever their orientation they will all have the same maximum slope which is that of the bank.

In more complex cases, two types of HRR are to be considered: spatial and temporal HRR. Here it is a question of considering variable speeds of displacement of different shorelines during a given flow reduction period. River island contours and right and left banks of various channels can present several types of slopes that may have different HRR. The temporal HRR is calculated globally (across the entire study reach) by dividing the average variation of the surface level elevation by the average maximum slope of the wetted surface. The spatial HRR is the average of the local HRRs weighted by their respective surface areas. Appendix 2 explains in more detail the difference between spatial and temporal HRR using a simplified case study.

In Equations (2) and (4) we consider here the part of the hydraulic mesh that has been flooded during the decrease in flow from *Q1* to *Q2* (*Q″1* in Figure 2). The index *i* refers to one of the cells that compose it.

Equation (2) uses in the denominator the average maximum slope of the bottom of the emerged part. This is calculated by averaging the maximum slopes of the bottom of the emerged cells weighted by their areas. Equation (2) uses the average variation of the water surface in the numerator; Figure 2 explains how this calculation is done.

Equation (4) calculates the spatial HRR by averaging the local HRR_i (Equation (3)) of the emerged cells weighted by their areas. The term $\Delta z_{surf,i}$ refers to the local variation in water level in the vicinity of the hydraulic cell of index *i*. This difference in water surface elevation must be that of the part of the hydraulic mesh that will remain in water during the flow reduction and that is locally close to the dewatered cell of index *i*. We consider that the water surfaces of these meshes that remain fully wetted are less prone to hydraulic aberrations than the edge meshes.

$$HRR_{temp}(Q1, Q2, \Delta t) = \frac{\Delta z_{surf}}{\left\{\frac{\sum[smaxb_i \cdot A_i]}{\sum A_i}\right\} \cdot \Delta t} = \frac{\Delta z_{surf}}{\Delta t} \cdot \frac{\sum A_i}{\sum[smaxb_i \cdot A_i]} \quad (2)$$

$$HRR_i(Q1, Q2, \Delta t) = \frac{\Delta z_{surf,i}}{\Delta t \cdot smaxb_i} \quad (3)$$

$$HRR_{spa}(Q1, Q2, \Delta t) = \frac{\sum[HRR_i \cdot A_i]}{\sum A_i} = \frac{1}{\Delta t} \cdot \frac{\sum\left[\frac{A_i \cdot \Delta z_{surf,i}}{smaxb_i}\right]}{\sum A_i} \quad (4)$$

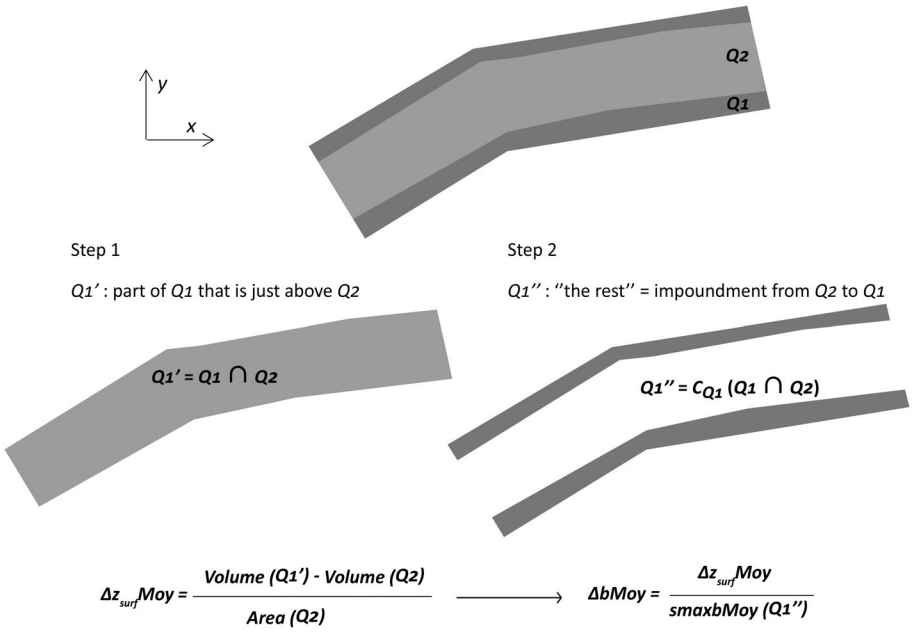

FIGURE 2 Illustration of the calculation of the average lateral displacement of the shoreline in the horizontal plane. For a flow reduction of a pair of discharges (*Q1* to *Q2*), the extraction of the emerged part of the hydraulic mesh during the flow reduction corresponds to *Q1″*, with the average variation of the water surface level being $\Delta z_{surf}Moy$, and with *smaxbMoy*(*Q1″*) being the average maximum slope of the river bottom. The calculation of $\Delta bMoy$ corresponds to the average lateral displacement of the shoreline in the horizontal plane

In reality, the calculation of the spatial HRR presents a numerical problem. If we imagine a stretch of several kilometers of river, and a dewatered cell with a perfectly horizontal bottom, the local value of the HRR_i is infinite and therefore this will also be the value of the spatial HRR. Even if we do not encounter any flat-bottomed cells, small portions of the dewatered bottom are close enough to horizontal to contribute to the majority of the final value of the spatial HRR. If one seeks to use this approach to construct metrics for environmental impact assessments, care must be taken to avoid this error that exaggerates the HRR (tends toward infinite values). For example, this can be done by using the median rather than the mean of the HRR_i, or by analyzing the distribution of the HRR_i and recalculating an average after eliminating the outliers.

From a mathematical perspective, the distribution of the proportional area of the HRR_i values is the most informative for understanding fish stranding; however, it remains to be determined how this can be interpreted biologically. Note that the mapping of HRR also allows us to locate the areas with the highest risk of stranding, which can be particularly useful to plan field observations, if the model still accurately represents current river morphology conditions. Spatial statistics such as those proposed by McGarigal and Marks (1995) can also be used to identify and classify risk areas. Similarly, the representativity of study sites (of an entire river reach) can be determined a priori.

The temporal HRR, which can be calculated by sub-reach, appears to be more easily used to calculate metrics and define indicators than the spatial HRR. If a threshold value is eventually established that should not be exceeded to minimize stranding impacts, the prevalence of local values significantly higher than the established threshold can be identified for study and/or mitigation. This remains to be evaluated with field and/or experimental studies.

If a threshold value for limiting the stranding of juvenile fish HRR_{fish} is chosen, since the average distance traveled by the shoreline in the horizontal plane is known by Equation (5), the recommended time interval Δt_{fish} to proceed from *Q1* to *Q2* will be defined by Equation (6).

$$\Delta b(Q1, Q2) = \frac{\Delta z_{surf}}{\frac{\sum [smaxb_i \cdot A_i]}{\sum A_i}} \tag{5}$$

$$\Delta t_{\text{fish}}(Q1, Q2) = \frac{\Delta b(Q1, Q2)}{HRR_{\text{fish}}} \tag{6}$$

The reduction gradient noted Grad(*Q1*, *Q2*, HRR_{fish}) [$m^3.s^{-1}.h^{-1}$] is calculated algebraically as follows in Equation (7). It is used in particular to indicate the variation in hourly discharge that must be respected in the flow range [*Q1*, *Q2*] to satisfy the HRR_{fish} management constraint.

According to the general hydraulic geometry power laws, variations in the width of the wetted bed can be related to variations in discharge (Leopold & Maddock Jr, 1953). When the flow increases, the value of the shoreline displacement gradient GradΔb (*Q1*, *Q2*) [$m/m^3.s^{-1}$] decreases (Equation 8), inversely, they increase the reduction gradient and the operational constraint is thus reduced.

$$\text{Grad}(Q1, Q2, HRR_{\text{fish}}) = \frac{Q1 - Q2}{\Delta t_{\text{fish}}(Q1,\ Q2)} \tag{7}$$

$$\text{Grad}\Delta b(Q1, Q2) = \frac{\Delta b(Q1, Q2)}{Q1 - Q2} \tag{8}$$

In practice, 2D hydraulic models are not designed for this kind of eco-hydraulic analysis, and two difficulties must also be overcome.

- From the original mesh, the dry cells as well as the dry parts of the "semi-wet" cells must be cut out (Figure 3).

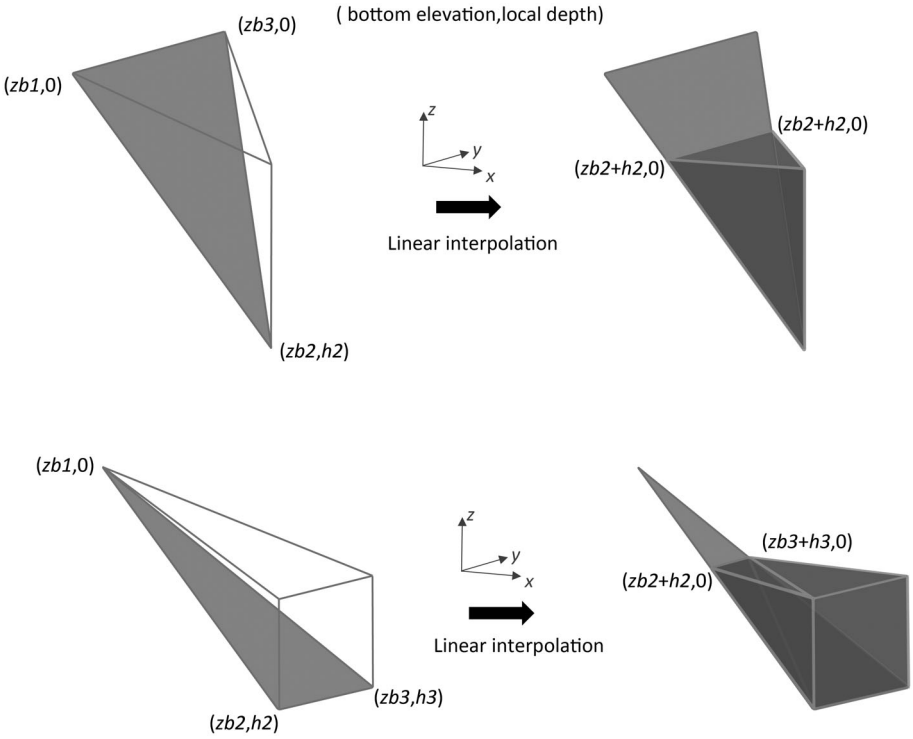

FIGURE 3 Illustration of two different cases where a partly emergent cell is partitioned into wet and dry cells, using the definition of the free surface water level obtained from the water vertical depths at the nodes of the triangle: (zb_i bottom elevations, h_i heights of water)

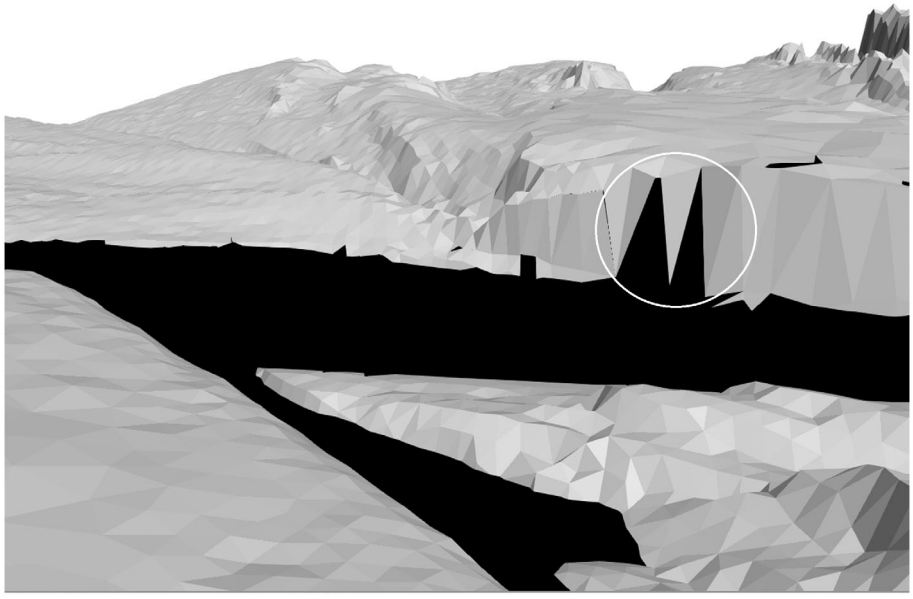

FIGURE 4 Illustration of an example of aberrations in the results of the hydraulic simulation regarding water levels (cf. circled zone) based on the visualization of a 2D hydraulic simulation with ParaView (vertical exaggeration X10); the darkened area is the water surface

- The hydraulic aberrations at the edge of the wetted area where wet cells "rise" on the banks must also be cut out (Figure 4).

Finally, it seems logical to perform calculations only in the part of the model mesh in which fish can realistically be found. If the minimum depth used by fish (according to the species and age/size of interest) is known, it is then possible to eliminate zones that are too shallow by cutting the meshes of *Q1* and *Q2* before extracting the dewatered zone. To set this minimum value, an analysis considering not only the biology, but also the quality of the hydraulic simulations is recommended, as the areas set aside may represent a substantial portion of total area (in some cases more than 10% of the surface area has a depth less than 1 cm; Le Coarer unpublished data). The minimum threshold thus has to be carefully defined and justified.

Furthermore, if the time and space intervals between the hydraulic simulations considered are not too large, and if the range of depths and velocities used by the target fish are known, it may be preferable then to only use the hydraulic part of *Q1* containing this hydraulic class to determine the HRR_i.

The workflow of HRR calculation includes seven steps.

1. Import of 2D hydraulic simulation results in a permanent or transitional regime. If necessary, transformation of finite volume mesh into triangular finite element mesh. The water surface elevation and the water depth should be given at the nodes defining triangular mesh. This is necessary to be able to split meshes into dry and wet parts by interpolation, and to calculate the water surface slope of each mesh to identify hydraulic aberrations.
2. Remove hydraulic aberrations of each simulation. An efficient way to perform this automatically is to eliminate the meshes at the edge of the wetted bed whose water surface slopes are beyond the standard deviation.
3. Cropping the dry and semi-wet cells, to keep only the wetted part of the simulations.
4. Extraction of dewatered areas by discharge pair of hydraulic simulation (*Q1*, *Q2*), the time intervals for each flow reduction must be known. For each discharge pair, the data are $smaxb_i$, the maximum slope of the bottom, $\Delta z_{surf,i}$ the local variation of the water level in the vicinity of the cell during the reduction and the HRR_i. The data at the nodes in addition to their coordinates (*x*,*y*,*zb*) also include the depths and depth-averaged velocities of the hydraulic simulation "*Q1*". These hydraulic values must be linearly interpolated when new nodes are created during the extraction.
5. Define hydraulic classes, crossing mean velocity and depth (e.g., such as hydrosignatures [Le Coarer, 2007]), then cut out parts of cells on the edge of the wetted bed in parts that are too shallow for the fish species/stages being considered. The depth limit for cyprinid fry in France is at least 1 cm (G Carrel, pers. comm).
6. Calculation of: Δz_{surf} (Figure 2) the mean variation of the water level, *smaxb* the average maximum slope of the river bottom, Δb the average distance traveled by the shorelines and finally the temporal HRR, per discharge pair. Using Equation 5 allows to recommend flow reduction duration time to prevent the risk of stranding (if an HRR threshold is known).
7. For each discharge pair, as hydraulic data has been registered at step-4, a habitat analysis available to juveniles prior to dewatering can be conducted.

To calculate average HRRs for the complex topology of a braided river, we propose to use 2D hydraulic modeling transformed if necessary in finite elements with a fixed triangular mesh. The HRR increases when the flow decreases linearly, so it must be calculated either between two stabilized flows or preferably between two-time steps in a transient regime (*Q1*, *Q2*). To calculate the "temporal" average HRR in a complex situation with islands and asymmetrical banks with complex shapes, we must divide the average distance traveled by the shoreline by the time interval elapsed during the flow decrease. We determine this average distance by dividing the average decrease in water surface level by the average slope of the bottom of the dewatered area.

HRR calculations, as outlined above, are based on 2-D hydraulic models. As of yet, no studies have linked measured or theoretical HRR values to specific fish stranding risk for any fish species in any actual rivers (Moreira et al., 2019). The ability to calculate this indicator will allow for eco- hydraulicians to test its utility as an indicator of fish stranding risk.

It is possible for the ecohydraulics community to test the HRR approach, as explained above, by using a specific HRR module added to the HABBY software (https://habby.wiki.inrae.fr/en:start) which is a free and open-source program. HABBY was developed to estimate ecological flows by hydraulic habitat suitability calculations, from external hydrodynamic model outputs. The Python code of the algorithms developed is available on GitHub (https://github.com/YannIrstea/habby) and a quick tutorial for HRR calculations is available on HABBY webpage. The only necessary data is the outputs of hydraulic models (Telemac 2D in the tutorial). The HRR module of the HABBY software should be used either to compute automatically HRR because no other solutions are currently available or either as reference for everyone who would want to develop their own solutions (to compare the outputs). HRR computation is completely independent of habitat model computations.

In HABBY, the indices of the original mesh common to all simulations are kept as information for every cell. And this is true whatever the operations of cutting or partitioning the cells. Moreover, for a given mesh, whether it is the original mesh or the mesh of a hydraulic unit, we can build a cell connectivity table. That is, the information for each cell in the mesh, of the indices of at most three cells that share common segments/node pairs with it. For the calculation of $\Delta zsurf_i$ or for the extraction of dewatered cells, these are the elements that allow the efficiency of the algorithms for finding neighboring cells in space and time.

Defining minimum depth is a necessary step to exclude cells or parts of cells that are biologically incoherent (because even the smallest fish would not be present in these areas). Once this minimum depth is decided (based on target species and life stages at risk and their behavior), it is necessary to split cells containing depths that are shallower than this threshold. To search for the node position (with depth equal to the threshold) to determine the new geometries, it is recommended to perform linear interpolation, which can most easily be done with a software solution (such as HydroSignature) but specific algorithms or code could also be developed and used.

To illustrate the computation and the outputs of the HRR calculations, we used a stream reach of the lower part of the river Durance which is a braided and highly regulated river from the Southeast of France, flowing from the Alps to the Rhône River. The water of this river is used for hydroelectricity production and water supply. The 16 km stream reach from this study encompassed several successions of hydrological units (from pool to riffles).

The methodology presented here is the result of research work carried out within the framework of a technical group charged with studying means to mitigate hydropeaking flows in a river reach of the lower Durance River in France (Le Coarer, Beguin, Reynaud, & Von Gunten, 2016). The lower part of the Durance, where the study site is located, is a large braided gravel-bed river, whose fish community consists mainly of rheophilic cyprinids.

3 | RESULTS

Table 1 presents an extract of this study for a 16 km linear section, nine discharges modeled with Telemac 2D. These results are presented for an arbitrary HRR_{fish} of 1 m/h (used as a theoretical cut-off value that is easy to calculate but that has no basis in the scientific literature). Assuming this arbitrary threshold, the time necessary to go from peak flow (259 $m^3.s^{-1}$) to the minimum baseflow (9.2 $m^3.s^{-1}$) was calculated to be more than 22 h.

Note in this example with a constant arbitrary HHR of 1 $m.h^{-1}$ during the decreasing flow event, the VRR could vary from 6.0 to 6.7 $cm.h^{-1}$, which corresponds to a variation of 11% (Table 1) over the 16 km river reach. To compare the spatial autocorrelation of VRR and HRR we computed the Moran's Index (*I*) for both variables and for each discharge pair. To do so, we defined adjacency matrices based on the nearest neighbors (surrounding cells). For computation reasons we only consider cells with HRR lower or equal to 10. Whatever the discharge pair, the Moran's Index was always greater for VRR than for HRR (Table 1), suggesting that two close cells tend to have more similar VRR values than HRR values. This pattern is also visible on Figure 5, with contiguous cells displaying close colors with the VRR, while the same cells could have different HRR values (different colors). At a larger spatial extent, VRR seems to vary mainly with the change of morphological units, HRR can vary much more locally depending of the complexity of the topography (Figure 5).

4 | DISCUSSION

Rapid decreases in discharge during hydropeaking events (from peak to base flow) are known to present risks of fish mortality from stranding and/or trapping. While not able to address all of the potential impacts that hydropeaking can have on fishes (via habitat modification, sediment mobility, thermal effects and trapping, among others), the approach of calculating HRRs appears to be pertinent for assessing juvenile fish stranding risk and warrants being tested in the field.

Many existing indicators, based on water height variation or surface area variation are proxies for the mechanism that drives stranding, whereas HRR is a direct descriptor of the stranding mechanism, as it calculates the velocity of the water receding from the shoreline. If this velocity is too high (thresholds to be determined), fish may not have sufficient time to find refuge toward the center of the channel and therefore it is more likely to become stranded in the dewatered habitat.

The HRR module of the HABBY software would enable a rapid first assessment of the HRR concept for the ecohydraulic community but also to conduct a spatial evaluation of stranding risk along the river reach map by mapping the local HRR versus time. This module should also be used as a reference for HRR computation to all who would compute HRR from the formulas presented in this manuscript. The HRR module accepts several 2D hydrodynamic models as inputs and further compatible models will be available in the future. Additionally, work is underway to improve the transition from finite volumes to finite elements.

Depending on the hydrodynamic model outputs (e.g., its resolution), before computing HRR, it is necessary to thoughtfully define minimum water depths which determine the wet/dry transition (1 cm in this example). If cells or part of cells are shallower than this threshold, they must be split to be removed from HRR computation. This step is essential (as is the ecological justification of the threshold chosen) because it substantially influences the results.

TABLE 1 Results of temporal Horizontal Ramping Rate (HRR) and Vertical Ramping Rate (VRR) calculations for a 16 km reach of the Durance River for eight discharge pairs (Q1, Q2), using an arbitrary HRR threshold value for increased risk of stranding of fish: HRR_{fish} of 1 $m.h^{-1}$

Q1 [$m^3.s^{-1}$]	259	175	150	110	76	60	48.4	25.5
Q2 [$m^3.s^{-1}$]	175	150	110	76	60	48.4	25.5	9.2
ΔQ [$m^3.s$]	84	25	40	34	16	12	23	16
smaxbMoy [%]	6.3	6.0	6.5	6.2	6.7	6.6	6.5	6.0
Δz_{surf} [m]	0.29	0.10	0.19	0.20	0.11	0.09	0.21	0.22
$Grad\Delta z_{surf}$ [$m/m^3.s^{-1}$]	0.4	0.4	0.5	0.6	0.7	0.8	0.9	1.4
Δb [m]	4.7	1.7	2.9	3.2	1.6	13	3.2	3.7
$Grad\Delta b$ [cm/ m^3s^{-1}]	5.5	6.9	7.3	9.5	9.8	11.5	14.2	22.5
Δt [h]	4.7	1.7	2.9	3.2	1.6	1.3	3.2	3.7
VRR [$cm.h^{-1}$]	6.3	6.0	6.5	6.2	6.7	6.6	6.5	6.0
$GradHRR_{fish}$ [$m^3.s^{-1}$ h^{-1}]	18.0	14.5	13.7	10.5	10.2	8.7	7.1	4.5
I HRR	0.497	0.518	0.555	0.542	0.525	0.553	0.544	0.515
I VRR	0.722	0.731	0.727	0.722	0.75	0.753	0.738	0.733

Note: The other variables mentioned are: smaxbMoy, the average maximum slope of the dewatered river bottom; Δz_{surf}, the variation of the water level; and $Grad\Delta z_{surf}$, its gradient per flow reduction; Δb, the average lateral displacement of the shoreline in the horizontal plane and $Grad\Delta b$ its gradient per flow reduction; Δt, the time interval; $GradHRR_{fish}$ the gradient of flow reduction per time interval; *I HRR* and *I VRR*, correspond to the Moran's index (statistic of spatial autocorrelation).

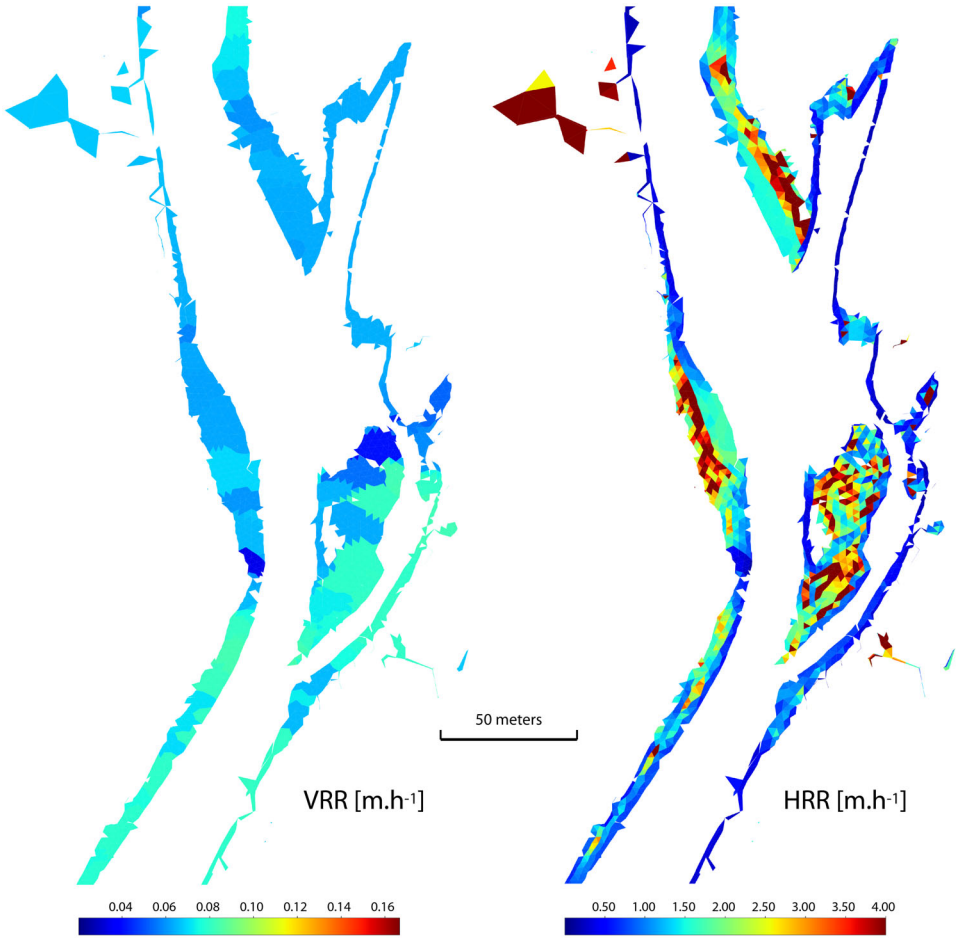

FIGURE 5 Vertical Ramping Rate (VRR) and Horizontal Ramping Rate (HRR) maps for a flow variation going from 35 to 9.2 $m^3.s^{-1}$ in 400 min [Color figure can be viewed at wileyonlinelibrary.com]

In addition, substrate is not considered in the modeling approach presented here, although it most certainly plays an important role in the stranding mechanism and in inter-peak survival of stranded fish. Theoretically, it would be possible to calculate a velocity of displacement of the shoreline on the bottom of the riverbed: Bottom Ramping Rate (BRR). This could be more relevant for qualifying the stranding risk of benthic species, but in this case, it is critical to account for substrate characteristics. It would also be useful to model exchanges with the alluvial water table, which can reduce the impact of stranding during hydropeaking events by increasing survival between peaking events.

No specific HRR thresholds for stranding have been presented in the literature. However, such values can be extrapolated from certain studies investigating VRR in fluvariums where sufficient geometry information exists to convert the two values. Following this, from the data provided by Halleraker et al. (2003) during his stranding experiment in fluvarium, we can estimate the HRR_{fish} corresponding to a VRR_{fish} of 0.1 $m.h^{-1}$. Using the width of the fluvarium channel and the dewatering time indicated in the experiment, we obtain a threshold value of 1.6 $m.h^{-1}$ in HRR_{fish} for juvenile trout in that particular configuration. Given the generally lower swimming capacity of cyprinid fry/juveniles as compared to salmonids, the HRR_{fish} threshold stranding values for cyprinids could be lower than for salmonids. However, research in different river types and for different species are necessary to determine whether threshold values can be established and make ecological sense in a given context.

We believe that field and fluviarium research is needed to better define the stranding risk of juvenile fish according to the HRR, temperature, substrate characteristics, nychthemeral cycles, species and size of individuals. Furthermore, research needs to be conducted to compare the relative risks and survival associated with stranding and trapping for different species and river morphological conditions. It is this knowledge that will lead to the best use of the HRR indicator in an overall risk-based approach aimed at reducing hydropeaking impacts (e.g., Barillier, Bêche, Malavoi, & Gouraud, 2021), in particular on fishes, but that could also be applied to other taxonomic groups at risk for stranding (e.g., aquatic insects, amphibians).

No single indicator of hydropeaking pressure can address all of the potential effects of hydropeaking on fishes or other aquatic organisms. The HRR, for example, is an indicator specific to stranding risk, but it does not explicitly consider trapping risks (e.g., resulting from connection-disconnection of secondary channels), or other hydropeaking impacts (on sediment mobility, habitat modification, water quality, etc). However, it does have the potential to be applied to similar situations in other aquatic ecosystems. For example, the HRR approach could be used to quantify potential ecological risks related to water level variations in artificial reservoirs that can create similar situations of dewatering as those encountered in hydropeaking rivers.

This modeling approach only has value, however, when coupled with local biological studies to evaluate risks.

Recent experiences have shown that it is generally difficult to assess the impact of hydropeaking at a population level because of interannual variations in natural hydrological conditions that have a predominant influence on population structure (Judes et al., 2020). Nevertheless, using the cumulative average distances traveled by the shorelines during the life span of the juvenile fish could also be tested as a metric to model fish densities as way to characterize hydropeaking influences, particularly when fish stranding is thought to be one the main sources of hydropeaking impacts on fish populations. This type of approach ultimately aggregates several types of information that influence stranding risk, such as river morphology, peaking amplitude, and down-ramping rates. It is worth noting, however, that depending on the local river morphology and species behavior, as well as specific hydropeaking operations, fish trapping may be a more important source of impacts than fish stranding. Site-specific reconnaissance and qualification of risk sources should therefore precede the implementation of any modeling approach.

This study presented a methodology to compute the HRR and highlighted the essential points to respect to assess it consistently. By making its computation relatively easy, future studies will be able to compare HRR with other hydropeaking characterization indicators. By doing this for different sites with different morphologies, and comparing them to observed stranding, it should be possible to evaluate the most appropriate indicator to use on a site-by-site basis, depending on the target species and their ecology, local hydromorphological conditions and the main source(s) of hydropeaking risk(s) (stranding, trapping, substrate mobility, …).

LIST OF SYMBOLS

$Q1$	River discharge before the flow reduction $Q1 > Q2$ ($m^3.s^{-1}$)
$Q2$	River discharge after the flow reduction $Q2 < Q1$ ($m^3.s^{-1}$)
Δt	Time interval during the flow reduction expressed in hours (Hr)
HRR	Horizontal ramping rate ($m.hr^{-1}$)
$HRR_{temp}(Q1, Q2, \Delta t)$	Temporal HRR ($m.hr^{-1}$)
$HRR_{spa}(Q1, Q2, \Delta t)$	Spatial HRR ($m.hr^{-1}$)
HRR_{fish}	HRR threshold value for increased risk of stranding of fish ($m.hr^{-1}$)
z_{surf}	Water surface level elevation (m)
Δb	Average lateral displacement of the shoreline in the horizontal plane (m)
$Grad(Q1, Q2, HRR_{fish})$	Hourly discharge reduction gradient to comply with the constraint HRR_{fish} ($m^3.s^{-1}.h^{-1}$)
$Grad\Delta b(Q1, Q2)$	Gradient of the average lateral displacement of the shoreline in the horizontal plane per flow reduction ($s.m^2$)
i	Index of a hydraulic cell
A_i	Area of a hydraulic cell of index i (m^2)
$smaxb_i$	Maximum slope of the bottom of the cell of index i ($m.m^{-1}$)
$\Delta z_{surf,i}$	Local variation of the water level in the vicinity of the dewatered cell of index i (m)
$z_{b,k}$	Bottom elevation of the node of index k (m)
h_k	Local water depth of the node of index k (m)
I	Moran's index (statistic of spatial autocorrelation)

ACKNOWLEDGMENTS

The authors thanks K. Jorde for his general recommendations of applicable methods in ecohydraulics during a workshop in Switzerland in 2016.

DATA AVAILABILITY STATEMENT

The data that support the findings of this study are available from EDF. Restrictions apply to the availability of these data, which were used under license for this study. Data are available from the author(s) with the permission of EDF.

ORCID

Yann Le Coarer https://orcid.org/0000-0001-6715-5216
Marie-Hélène Lizée https://orcid.org/0000-0003-4766-3840
Leah Beche https://orcid.org/0000-0003-3597-4748
Maxime Logez https://orcid.org/0000-0001-9843-0495

REFERENCES

Alanärä, A., & Brännäs, E. (1997). Diurnal and nocturnal feeding activity in Arctic char (Salvelinus alpinus) and rainbow trout (Oncorhynchus mykiss). *Canadian Journal of Fisheries and Aquatic Sciences*, *54*(12), 2894–2900.

Anderson, E. P., Jackson, S., Tharme, R. E., Douglas, M., Flotemersch, J. E., Zwarteveen, M., … Arthington, A. H. (2019). Understanding rivers and their social relations: A critical step to advance environmental water management. *WIREs Water*, *6*, e1381. https://doi.org/10.1002/wat2.1381

Barillier, A., Bêche, L., Malavoi, J. R., & Gouraud, V. (2021). Identification of effective hydropeaking mitigation measures: Are hydraulic habitat models sufficient in a global approach? *Journal of Ecohydraulics*, *6*, 172–185. https://doi.org/10.1080/24705357.2020.1856008

Bejarano, M. D., Jansson, R., & Nilsson, C. (2017). The effects of hydropeaking on riverine plants: A review. *Biological Reviews*, *93*(1), 658–673. https://doi.org/10.1111/brv.12362

Björnsson, B. (2001). Diel changes in the feeding behaviour of Arctic char (Salvelinus alpinus) and brown trout (Salmo trutta) in Ellidavatn, a small lake in Southwest Iceland. *Limnologica*, *31*(4), 281–288. https://doi.org/10.1016/S0075-9511(01)80030-X

Bradford, M. J. (1997). An experimental study of stranding of juvenile salmonids on gravel bars and in sidechannels during rapid flow decreases. *Regulated Rivers: Research & Management*, *13*, 395–401. https://doi.org/10.1002/(SICI)1099-1646(199709/10)13:5<395::AID-RRR464>3.0.CO;2-L

Bruno, M. C., Siviglia, A., Carolli, M., & Maiolini, B. (2013). Multiple drift responses of benthic invertebrates to interacting hydropeaking and thermopeaking waves. *Ecohydrology*, *6*, 511–522. https://doi.org/10.1002/eco.1275

Greimel, F., Schülting, L., Graf, W., Bondar-Kunze, E., Auer, S., Zeiringer, B., & Hauer, C. (2018). Hydropeaking impacts and mitigation. In S. Schmutz & J. Sendzimir (Eds.), *Riverine ecosystem management, aquatic ecology series* (Vol. 8, pp. 91–100). Cham: Springer. https://doi.org/10.1007/978-3-319-73250-3_5

Halleraker, J. H., Saltveit, S. J., Harby, A., Arnekleiv, J. V., Fjeldstad, H. P., & Kohler, B. (2003). Factors influencing stranding of wild juvenile brown trout (*Salmo trutta*) during rapid and frequent flow decreases in an artificial stream. *River Research and Applications*, *19*, 589–603. https://doi.org/10.1002/rra.752

Harby, A., Forseth, T., Ugedal, O., Bakken, T. H., & Sauterleute, J. (2016). A method to asses impacts from hydropeaking (chair). In *11th international symposium Ecohydraulics*. Melbourne, Australia: The University of Melbourne.

Hauer, C., Holzapfel, P., Leitner, P., & Graf, W. (2017). Longitudinal assessment of hydropeaking impacts on various scales for an improved process understanding and the design of mitigation measures. *Science of the Total Environment*, *575*, 1503–1514. https://doi.org/10.1016/j.scitotenv.2016.10.031

Hayes, D., Moreira, M., Boavida, I., Haslauer, M., Unfer, G., Zeiringer, B., Greimel, F., Auer, S., Ferreira, T., & Schmutz, S. (2019). Life stage-specific hydropeaking flow rules. *Sustainability*, *11*(6), 1547. https://doi.org/10.3390/su11061547

Hervouet, J. M. (2007). *Hydrodynamics of free surface flows: Modelling with the finite element method*. Chichester: John Wiley & Sons.

Irvine, R. L., Thorley, J. L., Westcott, R., Schmidt, D., & DeRosa, D. (2015). Why do fish strand? An analysis of ten years of flow reduction monitoring data from the Columbia and Kootenay rivers, Canada. *River Research and Applications*, *31*(10), 1242–1250. https://doi.org/10.1002/rra.2823

Judes, C., Gouraud, V., Capra, H., Maire, A., Barillier, A., & Lamouroux, N. (2020). Consistent but secondary influence of hydropeaking on stream fish assemblages in space and time. *Journal of Ecohydraulics*, *1–15*, 157–171. https://doi.org/10.1080/24705357.2020.1790047

Lamouroux, N., Augeard, B., Baran, P., Capra, H., Le Coarer, Y., Girard, V., … Tissot, L. (2018). Débits écologiques : la place des modèles d'habitat hydraulique dans une démarche intégrée. *Hydroécologie Appliquée*, *20*, 1–27. https://doi.org/10.1051/hydro/2016004

Le Coarer, Y. (2007). Hydraulic signatures for ecological modelling at different scales. *Aquatic Ecology*, *41*(3), 451–459.

Le Coarer, Y., Beguin, J., Reynaud, N., & Von Gunten, D. (2016). Études des habitats hydrauliques piscicoles soumis à éclusées: aide à la détermination des débits souhaitables en Basse-Durance. [Rapport de recherche] Commande EDF-CIH, IRSTEA Centre d'Aix en Provence, pp.66. ⟨hal-02605616⟩.

Leopold, L. B., & Maddock, T., Jr. (1953). *The hydraulic geometry of stream channels and some physiographic implications (252)*. Washington, D.C.: U.S. Government Printing Office.

Maaß, A. L., Schüttrumpf, H., & Lehmkuhl, F. (2021). Human impact on fluvial systems in Europe with special regard to today's river restorations. *Environmental Sciences Europe*, *33*(1), 1–13.

McGarigal, K., & Marks, B. J. (1995). *FRAGSTATS: Spatial pattern analysis program for quantifying landscape structure (gen. Tech. Rep. PNW-GTR-351)*. Portland, Oregon: U.S. Department of Agriculture, Forest Service, Pacific Northwest Research Station.

Moreira, M., Hayes, D. S., Boavida, I., Schletterer, M., Schmutz, S., & Pinheiro, A. (2019). Ecologically-based criteria for hydropeaking mitigation: A review. *Science of the Total Environment*, *657*, 1508–1522. https://doi.org/10.1016/j.scitotenv.2018.12.107

Office fédéral de l'environnement OFEV (2016). Eclusées-Mesures d'assainissement. Retrieved from https://www.bafu.admin.ch/dam/bafu/fr/dokumente/wasser/uv-umwelt-vollzug/schwall-sunk-massnahmen.pdf.download.pdf/UV-1701-f.pdf

Patterson, R. J., & Smokorowski, K. E. (2011). Assessing the benefit of flow constraints on the drifting invertebrate community of a regulated river. *River Research and Applications*, *27*(1), 99–112. https://doi.org/10.1002/rra.1342

Salmaso, F., Espa, P., Crosa, G., & Quadroni, S. (2021). Impacts of fine sediment input on river macroinvertebrates: The role of the abiotic characteristics at mesohabitat scale. *Hydrobiologia*, *848*(18), 4189–4209. https://doi.org/10.1007/s10750-021-04632-8

Saltveit, S. J., Halleraker, J. H., Arnekleiv, J. V., & Harby, A. (2001). Field experiments on stranding in juvenile Atlantic salmon (Salmo salar) and brown trout (Salmo trutta) during rapid flow decreases caused by hydropeaking. *Regulated Rivers: Research & Management*, *17*(4–5), 609–622. https://doi.org/10.1002/rrr.652

Schmutz, S., Fohler, N., Friedrich, T., Fuhrmann, M., Graf, W., Greimel, F., Höller, N., Jungwirth, M., Leitner, P., Moog, O., Melcher, A., Müllner, K., Ochsenhofer, G., Salcher, G., Steidl, C., Unfer, G., & Zeiringer, B. (2013) Schwallproblematik an Österreichs Fließgewässern – Ökologische Folgenund Sanierungsmöglichkeiten. BMFLUW, Wien Hydropeaking Impacts and Mitigation.

Schneider, M., & Kopecki, I. (2016). *Ecohydraulic investigations of hydropeaking: The role of river morphology (chair), 11th international symposium Ecohydraulics*. Melbourne, Australia: The University of Melbourne.

The Brisbane Declaration (2007). The Brisbane Declaration: Environmental flows are essential for freshwater ecosystem health and human well-being. In *In 10th International River symposium* (pp. 3–6). Brisbane, Australia.

Tuhtan, J. A., Noack, M., & Wieprecht, S. (2012). Estimating stranding risk due to hydropeaking for juvenile European grayling considering river morphology. *KSCE Journal of Civil Engineering*, *16*(2), 197–206. https://doi.org/10.1007/s12205-012-0002-5

How to cite this article: Le Coarer, Y., Lizée, M.-H., Beche, L., & Logez, M. (2023). Horizontal ramping rate framework to quantify hydropeaking stranding risk for fish. *River Research and Applications*, *39*(3), 478–489. https://doi.org/10.1002/rra.4087

APPENDIX 1: CALCULATION OF THE MAXIMUM SLOPE OF A TRIANGLE IN DIMENSION 3

Let a triangle 123 in the coordinate system (O*xyz*) calculate *smax*, its maximum slope (Figure A1).

The triangle 123 lies in a vector plane $\vec{P}[123]$ of equation:

$$\left(\overrightarrow{12} \wedge \overrightarrow{13}\right) \cdot \overrightarrow{OM} = 0$$
$$u \cdot x + v \cdot y + w.z = 0$$

With

$$\begin{vmatrix} (x2-x1) & (x3-x1) & x \\ (y2-y1) & (y3-y1) & y \\ (z2-z1) & (z3-z1) & z \end{vmatrix} = 0$$

$$u = (y2-y1) * (z3-z1) - (z2-z1) * (y3-y1)$$

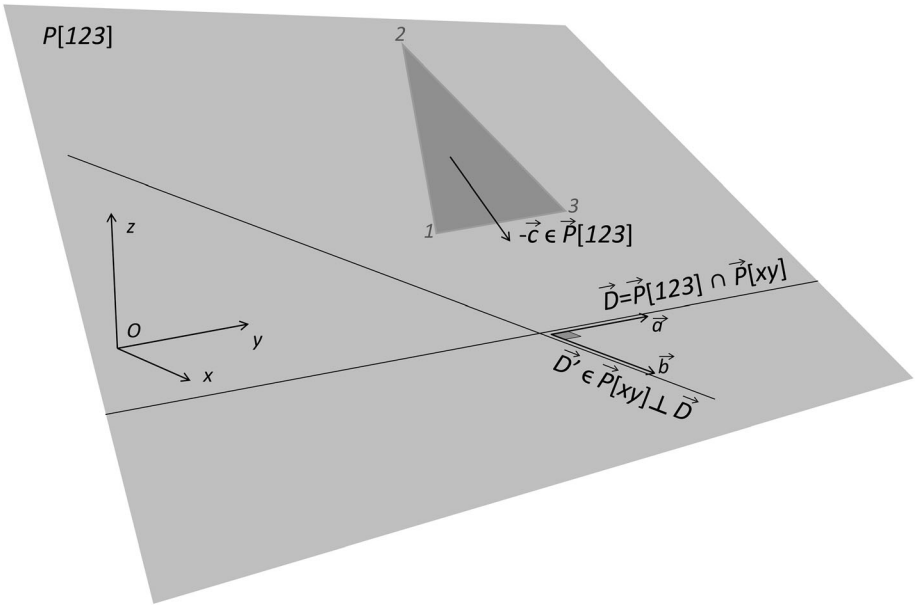

FIGURE A1 Calculation of the maximum slope of a triangle 1 2 3. *P*[*1,2,3*] is the plane containing the triangle, $\vec{D}$ is the vector line at the intersection of the vectorial plane $\vec{P}[123]$ with $\vec{P}[xy]$ being the horizontal plane, $\vec{D'}$ the vector line in the horizontal plane that is perpendicular to $\vec{D}$, and $-\vec{c}$ being the vector at the intersection of $\vec{D'}$ and $\vec{P}[123]$, which define the maximum slope of the triangle 1 2 3

$$v = (x3 - x1) * (z2 - z1) - (z3 - z1) * (x2 - x1)$$

$$w = (x2 - x1) * (y3 - y1) - (y2 - y1) * (x3 - x1)$$

We define $\vec{D}$ the vector line of intersection of $\vec{P}[123]$ with $\vec{P}[xy]$ the horizontal plane.

It checks.

$u \cdot x + v \cdot y + w.z = 0$ and $z = 0$

$$\vec{D}\, u \cdot x + v \cdot y = 0$$

In the horizontal plane $\vec{a}\begin{pmatrix} -v \\ u \\ 0 \end{pmatrix}$ is a direction vector of $\vec{D}$.

And

$\vec{b}\begin{pmatrix} u \\ v \\ 0 \end{pmatrix}$ is perpendicular to it and defines a line $\vec{D'}$ perpendicular to $\vec{D}$

$$\vec{D'} - v \cdot x + u \cdot y = 0$$

Let us define a vector $\vec{c}\begin{pmatrix} xc \\ yc \\ zc \end{pmatrix} \in \vec{D'} \cap \vec{P}[123]$

If we fix $yc = 1$ then $xc = \frac{u \cdot yc}{v} = \frac{u}{v}$ and $zc = \frac{-(u \cdot xc + v \cdot yc)}{w} = \frac{-\left(\frac{u^2}{v} + v\right)}{w}$

And we obtain the slope *smax* by $smax = \frac{|zc|}{\sqrt{xc^2 + yc^2}}$

$$smax = \frac{\left|\frac{-\left(\frac{u^2}{v} + v\right)}{w}\right|}{\sqrt{\left(\frac{u}{v}\right)^2 + 1}}$$

$$smax = \frac{\sqrt{u^2 + v^2}}{|w|}$$

Note: $w = 0$ in the case of a triangle in a vertical plane.

APPENDIX 2: TWO TYPES OF HRR: TEMPORAL (HRR_{temp}) AND SPATIAL (HRR_{spa})

The question: how to calculate the displacement velocity of the shoreline of a river reach whose flow decreases from *Q1* to *Q2* in a time interval Δt? We will call this displacement velocity Horizontal Ramping Rate (HRR).

Consider the case where we only consider the two steady-state simulations at *Q1* and *Q2*, and where we also consider that the variation Δz_{surf} of the surface water level is linear with time.

Let us choose the simple case of a uniform channel with symmetrical banks and two types of slopes, and study a portion of the cross-sectional profile for one of the banks that will be dewatered in 1 hour, going from *Q1* to *Q2* and for a vertical water level drop of 0.1 m. The calculations will be done for one linear meter of channel (Δs). In our case (Figure B1) the shoreline will have moved 1 m in 1 hour in the horizontal plane.

If we denote A_i the area of a cell *i* and $smaxb_i$ the maximum slope of the bottom of cell *i*, with HRR_i the local HRR of cell *i*; the two defining equations for temporal HRR (HRR_{temp}) and spatial HRR (HRR_{spa}) are:

$$HRR_{temp} = \frac{\Delta z_{surf}}{\left\{\frac{\sum [smaxb_i \cdot A_i]}{\sum A_i}\right\} \cdot \Delta t} = \frac{\Delta z_{surf}}{\Delta t} \cdot \frac{\sum A_i}{\sum [smaxb_i \cdot A_i]}$$

$$HRR_{spa} = \frac{\sum [HRR_i \cdot A_i]}{\sum A_i} = \frac{\sum \left[\left(\frac{\Delta z_{surf}}{\Delta t \cdot smaxb_i}\right) \cdot A_i\right]}{\sum A_i} = \frac{\Delta z_{surf}}{\Delta t} \cdot \frac{\sum \left[\frac{A_i}{smaxb_i}\right]}{\sum A_i}$$

If we express the areas in [m^2], the difference in altitude in [m] and the time in hours, the results in [$m.h^{-1}$] are:

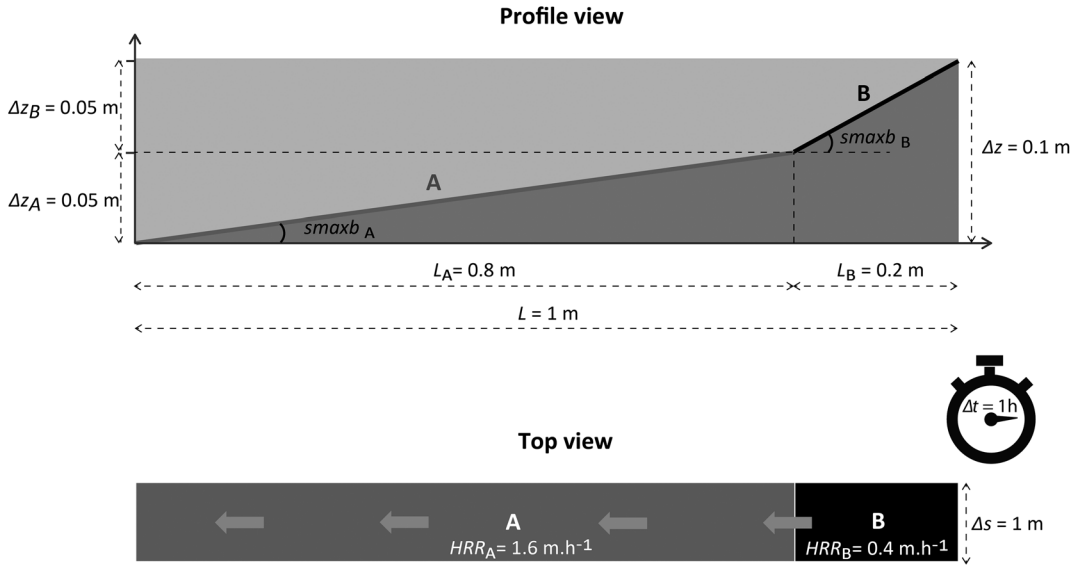

FIGURE B1 Illustration of a Horizontal Ramping Rate calculation along a bank with two different slopes. The bank (comprised of zones A and B) is dewatered over a one-hour time interval (Δt), over a portion of a cross-sectional profile of one linear meter of channel (Δs) and having a 1 m width (L), and for a total vertical water level drop of 0.1 m (Δz)

$$HRR_{temp} = \frac{0{,}1}{\left\{\frac{\frac{0.05}{0.2}\cdot 0.2\cdot 1+\frac{0.05}{0.8}\cdot 0.8\cdot 1}{0.2\cdot 1+0.8\cdot 1}\right\}\cdot 1} = 1\,m\cdot h^{-1}$$

$$HRR_{spa} = \frac{0.1}{1}\cdot\left[\frac{\left(\frac{0.2\cdot 1}{\frac{0.05}{0.2}}\right)\cdot+\left(\frac{0.8\cdot 1}{\frac{0.05}{0.8}}\right)}{0.2\cdot 1+0.8\cdot 1}\right] = 1.36\,m\cdot h^{-1}$$

For the temporal HRR_{temp} we find the value of 1 m.h^{-1} which corresponds to the displacement of shoreline. If we observe the phenomenon on a spatial scale, the HRR_{spa} per mesh are $HRRA = 1.6$ cm.h^{-1} and $HRRB = 0.4$ m.h^{-1}; these are displacement velocities of the shoreline per cell. For a given cell, the calculation takes into account the maximum slope of the mesh and the hourly rate of descent of the water surface $\left(\frac{\Delta z_{surf}}{\Delta t}\right)$ is assumed to be constant.

By calculating $HRR_i = \frac{\Delta z_{surf}}{\Delta t \cdot smaxb_i}$, this gives the velocity of shoreline retreat when the water level reaches the cell and the shoreline "sweeps" the cell, which occurs for each cell over a period of time less than the total duration of the dewatering in our case.

For our example, if a velocity of 1 cm.h^{-1} was a limit above which juvenile fish could be stranded, stranding could occur in cell A (1.6 m.h^{-1}) at the beginning of the dewatering, even though the temporal HRR would meet a set point of 1 m.h^{-1}.